Biointerface Research in Applied Chemistry
Open-Access Journal (ISSN: 2069-5837)

Article
Volume 13, Issue 1, 2023, 46
https://doi.org/10.33263/BRIAC131.046

Smaller Sized Hepatitis E Virus ORF2 Protein-Chitosan Nanoemulsion Conjugate Elicits Improved Immune Response

Dibya Rani [1], Baibaswata Nayak [2], Sudha Srivastava [1,*]

[1] Department of Biotechnology, Jaypee Institute of Information Technology, Noida- 201309, Uttar Pradesh, India; dibyajha0108@gmail.com (D.R.); sudha.srivastava@jiit.ac.in (S.S.);
[2] Department of Gastroenterology, All India Institute of Medical Sciences, Ansari Nagar, New Delhi- 110029, India; baibaswat@gmail.com (B.N.);
* Correspondence: sudha.srivastava@jiit.ac.in (S.S.);

Scopus Author ID 57209007229

Received: 30.10.2021; Accepted: 15.12.2021; Published: 30.01.2022

Abstract: Comparative evaluation of immunomodulating efficiency of chitosan nanoemulsion and gold nanoparticles as an adjuvant for truncated HEV ORF2 structural proteins (26 kDa or 54 kDa) were analyzed. Hepatitis E virus (HEV) ORF2 structural protein has been reported to be immunogenic in nature. In the present study, we have used truncated forms of structural protein-containing C-terminus neutralization epitope as a vaccine candidate. A high-energy emulsification process synthesized chitosan nanoemulsions. HEV antigens were encapsulated in chitosan nanoemulsion (CNE26, CNE54). Swiss albino mice were immunized with these nanoconjugates, and their potency to stimulate humoral immune response as well as cell-mediated immune response was evaluated. The humoral response in mice immunized with CNE26 nanoconjugates was found to be 2.7 times that of IFA26 immunized group, while larger protein nanoconjugate (CNE54) and gold nanoconjugates displayed immune response comparable to that of IFA26 and IFA54. Furthermore, a slower rate of antibody formation was observed in the case of GNP26 immunized mice as compared to GNP54 ones, emphasizing the effect of the size of nanomaterials/nanoconjugates on the immune response. At the same time, the effect of surface functionalization and inherent immune modulation property of chitosan nanoemulsion was observed for CNE nanoconjugates. Both gold and chitosan nanoconjugates elicited cell-mediated immune response as well in mice. This study suggests that smaller-sized protein antigen-chitosan nanoemulsion conjugate has higher immunological potential and can be a better future vaccine candidate than gold nanoparticles.

Keywords: chitosan; gold; nanoconjugates; immune adjuvants; Hepatitis E virus; vaccine.

1. Introduction

Viral hepatitis is the eighth leading cause of death worldwide (~1.44 million deaths) [1]. Hepatitis E virus (HEV) in general has a low mortality rate (0.5-3%) due to the self-clearing nature of the virus; however, mortality rates are much higher in immunocompromised patients, pregnant females (25%) [2] and patients with chronic liver diseases (27%) [3,4]. Lack of WHO-approved HEV vaccines calls for immediate efforts towards developing safe and efficacious vaccines to decrease mortality and morbidity [5,6].

Traditional methods of vaccine development (live attenuated or killed vaccine) have failed in the case of HEV because of the lack of a robust cell culture system. These limitations

shifted attention towards recombinant proteins as a vaccine candidate. Compared to the traditional (life attenuated or killed/inactivated organism) vaccine, recombinant proteins as immunogens are safer but weak immunogen and susceptible to degradation. Hence, they require an adjuvant that helps enhance immunogenicity and acts as a delivery system that provides protection [7]. Up until now, aluminum-based adjuvants have been extensively used but have their side effects [8,9]. Nanomaterials have emerged as a plausible alternative with intrinsic immunomodulatory functions as immune potentiators [10]. The robust immune response can be elicited by modulating the surface/morphology of nanoparticles such that they mimic the biophysical and biochemical characteristics of pathogens [11]. Polymeric nanoparticles - chitosan nanoparticles [12–17], Poly (lactide-co-glycolide) [18,19], Polycaprolactone [20], liposomes [21] and metallic gold nanoparticles (GNP) [22–24], iron oxide nanoparticles [25] have been extensively studied.

Initial mice experiments indicated the non-immunogenic nature of GNP [26–29]; however, Scott and co-workers showed their size-dependent immunogenic behavior [26]. Further studies have revealed both the size and morphology of the nanoparticles as crucial parameters in deciding their fate (elimination/clearance or phagocytosis) and pathway/mechanism of the immune response [30,31]. Smaller-sized GNP (<5 nm) have been reported as non-immunogenic, while GNP greater than 10 nm elicit both cells mediated as well as a humoral immune response [30,32,33]. Furthermore, Wang *et al*. showed that *in-situ* synthesized nanoclusters of antigen aggregates with GNP displayed a better immune response than antigen aggregates alone [34]. GNP's biocompatible, nontoxic, and immunogenic nature makes them a promising candidate for vaccine development [23,35–37]. In addition to this, surface modification resulted in improved transfection as well as an immune response [38].

In our recently published work on the immune response of GNP conjugated truncated ORF2 proteins of HEV, we observed that larger-sized proteins with additional neutralizing epitopes displayed better immune responses [39]. For further enhancement of immune response, one needs to understand – 1) whether antigen immobilization on the surface of gold nanoparticles is the most effective method or encapsulation within nanoparticles would yield a better response? 2) The choice of the nanomaterial itself can be a better adjuvant and immune response enhancer. Hence, we explored chitosan as the candidate material for encapsulation and immune response studies since it is a biodegradable, biocompatible, nontoxic biopolymer with high entrapment or encapsulation efficiency [40]. Chitosan increases the uptake and presentation of antigen by antigen-presenting cells [41] as well as protects the antigen [8,9,36,37,42,43]. The highly viscous nature of chitosan is, in fact, a blessing for prolonged retention at the site of injection, thereby eliciting improved immune response [44].

Present work describes the comparative evaluation of chitosan and gold nanoconjugates of truncated HEV capsid proteins (26kDa and 54kDa) as an immunostimulant. The immune response of nanoconjugates was further compared with Incomplete Freund's adjuvant (IFA, control) in terms of anti-HEV antibody generated in immunized mice as well as splenocytes proliferation in the presence of HEV protein. IgG titers of anti-HEV antibodies in GNP54 and chitosan nanoemulsion conjugated with smaller protein (CNE26) immunized mice were significantly higher than IFA54 or IFA26.

2. Materials and Methods

2.1. Synthesis of chitosan nanoemulsion by high energy emulsification method.

High energy emulsification process was employed to synthesize oil-in-water chitosan nanoemulsion as reported in our earlier work [45]. Chitosan solution (0.1%) was added to a mixture of Pluronic F127 (surfactant) and olive oil, and high energy ultrasonic waves (using ultrasonic probe sonicator) resulted in emulsification. This was followed by the dropwise addition of glutaraldehyde as a cross-linking agent while sonicating the mixture continuously. Finally, chitosan nanoemulsion was collected by centrifugation at 9000 rpm for 12 minutes.

Characterization of chitosan nanoemulsions was done by UV-Visible spectroscopy, while the hydrodynamic size and zeta potential of particles were measured by dynamic light scattering (DLS) technique.

2.2. CNE-protein nanoconjugate formation.

Two different truncated forms of HEV ORF2 were cloned in the pET30b (aa112-606 and aa 368-606) vector and expressed in BL21 (DE3) *E.coli* cells as 26 kDa and 54 kDa proteins (details can be seen in our previously published work [45]). These proteins were then purified using Ni-NTA affinity chromatography [45].

The purified proteins (26 kDa and 54 kDa) were then used for nanoconjugate formation with chitosan nanoemulsion by taking equal amount (400 µg CNE+400 µg of 26 kDa; 400 µg CNE+400 µg of 54 kDa) and incubating overnight at 4°C while stirring continuously. Henceforth, nanoparticles were separated by centrifuging at 9000 rpm under ambient conditions for 15 minutes. Pellet was washed 2-3 times with MilliQ water, and supernatants were pooled. The percentage of protein encapsulated in CNE, was estimated indirectly by calculating the amount of protein in the supernatant using Bradford assay as described in our previous work [39]. Nanoconjugation was further confirmed by dynamic light scattering and zeta potential measurements.

Vaccine nanoformulations were prepared by resuspending the nanoconjugates in 0.01 M phosphate buffer saline, pH 7.4. The volume of PBS to be added is decided based on the amount of protein immobilized on nanomaterials, such as 30 µg of protein per 200 µL of the formulation. These nanoformulations were named CNE26 and CNE54 depending on the size of the protein antigen used. In addition to these nanoformulations, IFA was also used as a positive control for the study. Vaccine formulation for the same was prepared by mixing IFA and 26 kDa and 54 kDa protein in a 1:1 ratio (w/w).

2.3. Institute animal ethical committee approval.

To perform studies on mice, scientific intent was approved and reviewed by Institutional Animal Ethics Committee (IAEC), AIIMS, New Delhi, for biosafety and animal ethical clearance. The reference number for the same is IAEC No. 160/IAEC-1/2019. Central Animal Facility (CAF), All the experimental procedures on mice were carried out strictly as per the guidelines, and experiments were planned to minimize the suffering of animals. Studies were also reviewed and approved by Institutional Biosafety Committee(IBSC), JIIT, Noida.

2.4. Selection of mice and their maintenance inside animal house.

Healthy inbred six to eight-week-old male swiss albino mice were used to perform immune response studies in mice purchased from CAF, AIIMS New Delhi, India. Mice were maintained properly in an air-conditioned room at 22°C temperature inside the microisolator cage with husks for bedding in a well-ventilated animal caging system in a laboratory (12-hour day/12 hour night cycle, and 50%-60% humidity) provided with biosafety level 3, in pathogen-free conditions and were observed every day for their well-being.

2.5. Experimental design for immunization.

Thirty-six, 6-8 weeks old swiss albino mice were taken for immunization study and were divided into six groups with six mice in each group. All mice in groups I, II, and III received CNE26, CNE54, and CNE only while groups IV, V, and VI served as positive control and were immunized with IFA26, IFA54, and IFA only, respectively. Each mouse was injected intramuscularly with a vaccine formulation of 0.2 mL followed by a booster dose on day-21 and day-35. Mice in each group were immunized with nanoconjugates formulations in the hind leg on day-0 (primary immunization), day-21 (first booster), day-35 (second booster), respectively.

2.6. Collection of a blood sample for immunological assays.

Mice were bled retro-orbitally to collect blood samples before immunization on day-0, before the first booster dose (day-21), before the second booster dose (day-35), and on day-42 before sacrifice. Isoflurane was used to anesthetize mice before taking blood samples. This was followed by centrifugation of blood samples at 800 × g for 5 minutes to separate serum. Isolated serum was stored at -20°C for further use in enzyme-linked immunosorbent assay (ELISA). Furthermore, mice were sacrificed on day-42, and dissection was performed to collect the spleen of each mouse. The collected spleen was further processed to perform splenocytes proliferation studies. For proliferation studies, splenocytes were incubated with purified truncated HEV ORF2 proteins.

2.7. Quantification of antibody in serum.

Serum samples collected before the start of immunization and each before booster dose were tested for the presence of anti-HEV IgG by enzyme-linked immunosorbent assay (ELISA) (Diapro, Diagnostic Bioprobes SRL, Italy). Samples were prepared by diluting the serum in the sample diluent (2% casein, 10 mM sodium citrate buffer, 0.1% Tween 20, 0.09% sodium azide) provided with the kit. Diluted serum samples, positive control, and negative control were added in microwells precoated with HEV-specific recombinant antigen and incubated for 1 hour at 37 °C. After incubation, microwells were washed thrice with 10 mM PBST buffer (10mM PBS, pH 7.4 + 0.05% Tween 20) followed by incubation with goat anti-mouse IgG HRP conjugate prepared in 5% BSA (1:5000 dilution) and again incubated at 37 °C for 1 hour. This was followed by washing thrice for 20-30 seconds each, followed by tetra-methyl-benzidine chromogen (100 mL) incubation for 20 minutes. The reaction was stopped by adding 100 mL of 0.3M sulphuric acid. Absorbance measurement at 450 nm using an ELISA reader was carried out to estimate the complex. If the ratio of sample$_{OD450}$/cut-off value is > 1.2, means mice, serum shows an increase in antibody titer, hence positive result.

2.8. Splenocytes proliferation assay.

The spleen was collected by sacrificing mice on day-42 of the experiment for splenocyte proliferation assay. The freshly removed spleen was washed in phosphate buffer (0.01M, pH 7.4) and cut into small pieces, and further teasing apart was done using the needle. These pieces were then passed through a sterile cell strainer (70 µm) followed by centrifugation at 1500 rpm at 4°C for 10 minutes. Splenocytes were collected in complete media RPMI1640 with 10% Fetal Bovine Serum and 100 U/mL penicillin-streptomycin. The pellet containing red blood cells(RBC) was lysed using 1X RBC lysis buffer, Thermo Fisher Scientific. Pellet was washed and resuspended in RPMI1640 media. Single-cell suspension of splenocytes was seeded in triplicates in a 96-well plate. This was followed by stimulation with 20 µg/ml (concentration optimized) of truncated HEV ORF2 26 kDa and 54 kDa protein. Cells treated with concanavalin A (ConA) served as positive control, while unstimulated cells and RPMI1640 media alone served as negative control and blank, respectively. After two days, [3-(4,5-dimethylthiazol-2-yl)-5-(3-carboxymethoxyphenyl)-2-(4-sulfophenyl)-2H-tetrazolium, inner salt] MTS assay was performed, and stimulation index was evaluated as $SI = \frac{OD_{Sample} - OD_{Blank}}{OD_{Negative} - OD_{Blank}}$, where OD is optical density.

3. Results and Discussion

3.1. Chitosan nanoemulsion

Chitosan nanoemulsions were characterized by UV-Visible absorption spectroscopy (see Figure 1). Figure 1 shows the absorption spectra of chitosan solution (solid black line) with λ_{max} at 295 nm. The successful synthesis of chitosan nanoemulsion using high energy emulsification process was marked by a shift in absorption maxima to lower wavelength 280 nm (Figure 1, dotted red curve).

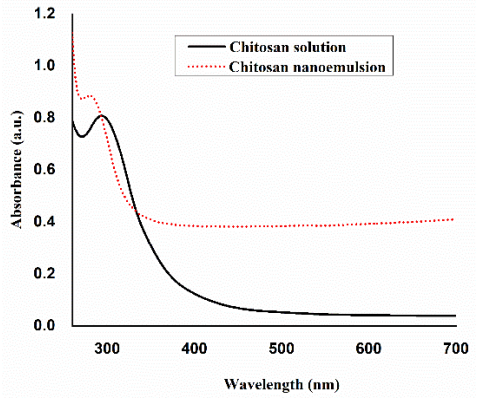

Figure 1. UV-Vis absorption spectra of Chitosan nanoemulsion (red dotted curve) and chitosan solution in acetic acid (black solid curve).

These chitosan nanoemulsions were further characterized using DLS. DLS measurements displayed an average size of 500 nm with 92% of the 200-850 nm particles, and 8% were of smaller size 78-190 nm (see Figure 2 (a), black solid line). On incubation of CNE with 26 kDa and 54 kDa protein, a marginal increase in size was observed with an average diameter of 530 nm. Figure 2 (a), the red-colored dashed curve shows 84% of CNE26 particles of 275-850 nm and remaining 16% were of 100-250 nm size. CNE54 exhibited almost the same size distribution as CNE26 with 80% particles between 280-950 nm and 20% of 100-250 nm

(Figure 2 (a), blue dotted curve). Also, Zeta potential of CNE was found to be -20.4± 1.1 mV (Figure 2 (b)) that reduced slightly after immobilization of proteins CNE26 (-18± 0.6 mV) (Figure 2 (c)) and CNE 54 (-19.3± 0.8 mV) (Figure 2 (d)).

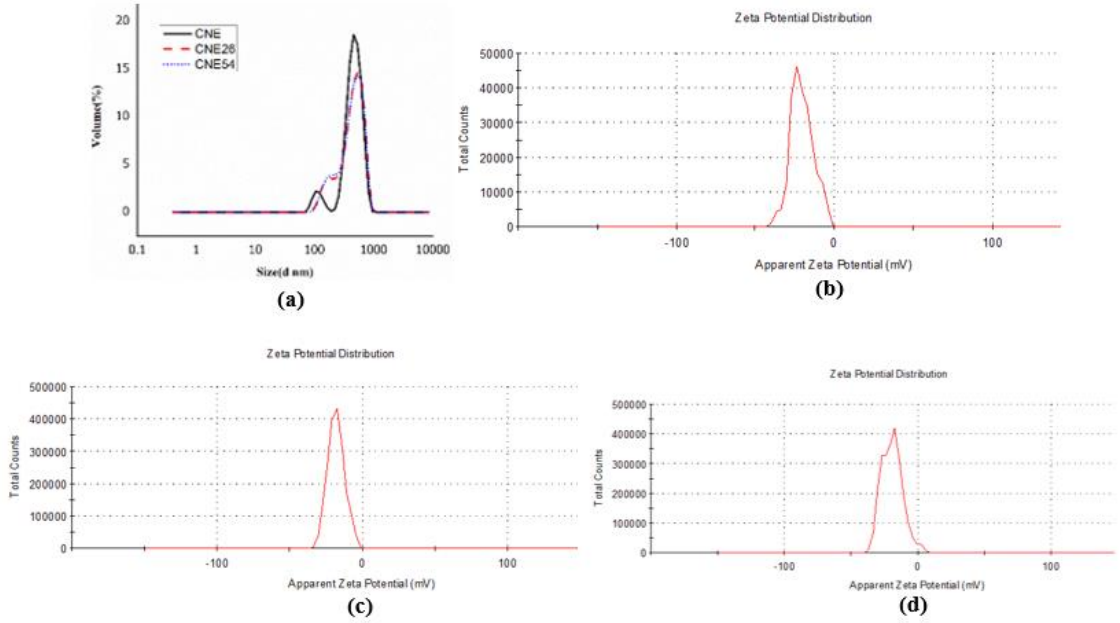

Figure 2. Dynamic light scattering measurement showing (a) size distribution of chitosan nanoemulsion (solid black line), after immobilization of 26 kDa (red dashed curve) and 54 kDa (blue dotted curve) proteins and zeta potential of (b) chitosan nanoemulsion (c) CNE26 and (d) CNE54.

3.2. Nanoconjugates mediated IgG antibody response.

Humoral immune response was evaluated after immunization of swiss albino mice with chitosan nanoconjugates. Nanoconjugates of 26 kDa and 54 kDa HEV proteins were prepared by incubating with CNE nanoemulsion (~500 nm). The loading efficiency of 26 kDa and 54 kDa protein on CNE (encapsulation+surface adsorption) was estimated to be 70% and 60%, respectively. As discussed above, the size of CNE was not much affected by protein encapsulation/adsorption.

The immune response elicited by chitosan (CNE26, CNE54) nanoconjugates were compared with the response of control IFA conjugates (IFA26, IFA54) and gold nanoconjugates (GNP26, GNP54) reported in a previous study [39]. All mice taken for the study were screened for HEV infection before immunization (day-0) using an anti-HEV ELISA kit. Mice having antibody titer ($sample_{OD}$/cut-off) lower than 1.2 were considered negative for HEV titer and included in the study. Figure 3 (a) shows antibody titer in mice serum before - primary immunization (day-0), a first booster dose (day-21), a second booster dose (day-35), and before sacrificing (day-42) of mice immunized with chitosan nanoconjugates. As shown in Figure 3 (a), at day-0, all mice had antibody titers below cut-off 1.2 (red-colored dotted line). None of the $sample_{OD}$/cut-off ratio data of mice immunized with CNE only formulations show seroconversion on day-21, day-35, or day-42. While CNE nanoconjugates, GNP nanoconjugates, and IFA-antigen conjugates formulations showed a slight rise in the antibody titers at day-21 after primary immunization (see Figure 3 (b) black boxes). In addition, 14 days post first booster dose (day-35, red-colored boxes) and 7 days after second booster dose (day-42, blue-colored boxes), anti-HEV antibody titers displayed an increasing trend. The increase in antibody titer with time confirms the specificity of anti-HEV antibodies. Figure 3 (b) shows

the relative antibody titer of day N (N=21, 35, 42) compared to day 0. The rate of increase in antibody titer in the case of CNE26 immunized mice was maximum, followed by GNP54, while in another group of mice immunized with GNP26, CNE54, IFA26, and IFA54 initial rate of increase were observed to be slower.

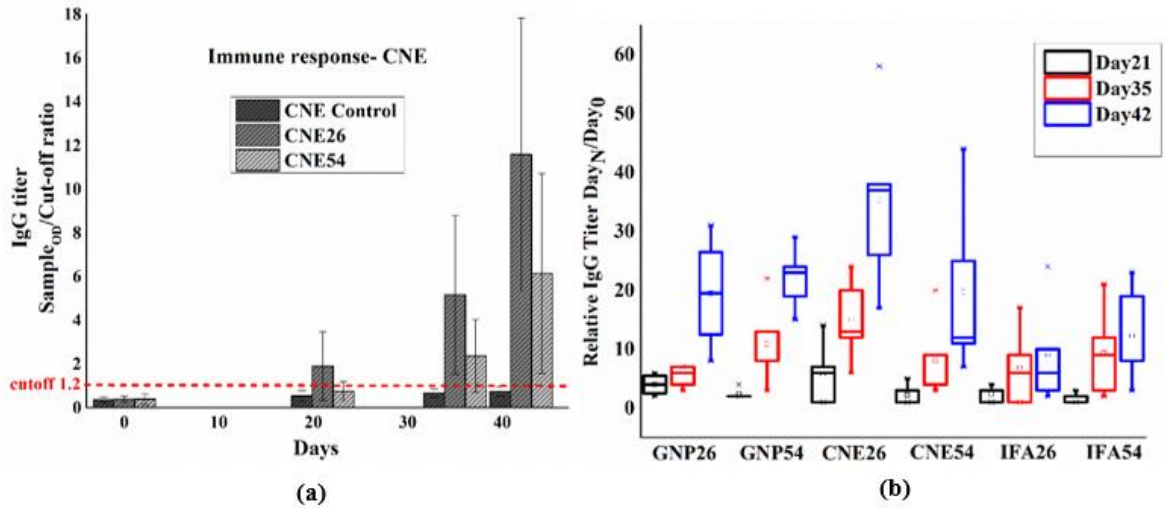

Figure 3. Result of ELISA showing anti-HEV antibody titer after immunization of mice with (a) CNE only, CNE26 and CNE54 nanoconjugates and red dotted line show sample$_{OD}$/cut-off value of 1.2 (Data presented as mean±SD). (b) Relative IgG titer at Day$_N$/Day$_0$ (Where N=day-21, 35, 42) of GNP26, GNP54, CNE26, CNE54 nanoconjugates, and IFA26 and IFA54 conjugate immunized mice.

3.3. Splenocytes proliferation as cell-mediated immune response.

All mice were sacrificed seven days after the second booster dose and dissected to collect spleen to analyze the cellular immune response. Single-cell suspension of splenocytes prepared from the spleen of all mice was induced for proliferation by incubating in the presence of purified 26 kDa and 54 kDa HEV ORF2 proteins. Evaluation of *in vitro* proliferation of isolated splenocytes was done in terms of stimulation index by performing MTS assay. Effect of purified HEV ORF2 protein on the proliferation of splenocytes was observed by seeding single-cell suspension in triplicate in a 96- well microplate and incubating at 37 °C, CO_2 incubator.

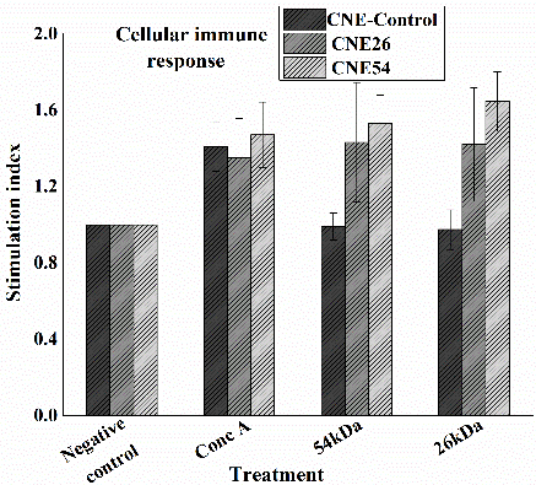

Figure 4. Stimulation index showing proliferation of splenocytes of CNE nanoconjugates immunized mice (Data presented as mean±SD).

Among the cultured cell, splenocytes treated with purified HEV ORF2 protein antigen served as a test group, untreated splenocytes as a negative group, concanavalin A (con A) treated cells as a positive control. Figure 4 shows the stimulation index for CNE26 and CNE54 group immunized mice when incubated in the presence of HEV ORF2 proteins. The stimulation index value of nanoconjugates formulation treated mice was comparable to that of positive control-treated mice splenocytes SI value while the negative group doesn't show proliferation. All data were found to be statistically significant ($p<0.05$) by one-way ANOVA test.

3.4. Discussion.

After the second booster dose, i.e., on day-42, mice immunized with CNE26 displayed 2.7 times higher IgG antibody titers than IFA26 immunized mice, while comparable levels of titers were observed in the case of CNE54 and IFA54. In addition to this, CNE26 exhibits a 1.9 times stronger antibody response than CNE54. Since the size of CNE26 and CNE54 is almost the same, the difference in immune response may be due to the antigen itself and/or surface properties of chitosan nanoconjugates. However, IFA and GNP conjugates displayed opposite trends, i.e., higher antibody response in 54 kDa conjugates than 26 kDa conjugates. Mice immunized with GNP54 nanoconjugates displayed 1.4 times higher IgG titers than those who received GNP26 nanoconjugates. As reported in our previous study [39], this could be due to the presence of an additional neutralizing epitope in 54 kDa protein. The question arises, why CNE54 is then eliciting a lower antibody response than CNE26?

To answer the above question, one needs to understand – 1) the effect of size of nanoconjugates, 2) effect of nanomaterial itself in addition to 3) antigen size, neutralizing epitopes, and hydrophobic characteristics.

Inspection of the size of GNP and CNE nanoconjugates shows the approximately same size (530 nm) CNE26 and CNE54 while the size of GNP54 (100 nm) is greater than that of GNP26 (15 nm). The size of the immobilized protein - 26kDa and 54 kDa did not affect the size of chitosan nanoconjugates, probably due to the encapsulation of proteins inside the CNE and limited proteins on the surface CNE. While in the case of gold nanoparticles, proteins are on the surface, and 54 kDa protein is more hydrophobic than 26 kDa protein, hence greater interaction or more agglomeration leading to larger sized GNP54 conjugates as opposed to GNP26. Shukla *et al*. reported 3 nm gold nanoparticles to be non-immunogenic and are eliminated from the body [32]. Other studies have shown that GNPs larger than 10 nm elicit an immune response that is size-dependent and increases with an increase in size [46–48]. Lacerda *et al*. 2009, reported that larger-sized GNP could adsorb more serum proteins and other molecules present in blood compared to smaller-sized GNP having larger curvature forming "corona" and eventually eliciting immune response [49]. Furthermore, Chen *et al*. reported that peptide-modified GNP are taken up by dendritic cells more effectively and can process vaccine peptides and generate immune response [50]. In light of the above facts, the enhanced IgG titers for mice immunized with GNP54 could be attributed to the larger size of GNP54 and/or due to the presence of additional neutralizing epitope in 54 kDa protein as opposed to 26 kDa.

CNE response can be understood in terms of physiochemical and immunomodulating properties of chitosan rather than the size of nanoconjugates or proteins. Zaharoff *et al*. reported that due to the high viscosity of chitosan, 60% of antigen proteins stay at the injection site for a week [44]. In addition to this, chitosan also results in cellular expansion and inflammation of nearby lymph nodes for nearly two weeks till chitosan degrades, thereby generating an adaptive

immune response. This could be due to the immunogenic nature of chitosan and receptor-mediated phagocytosis [51]. This explains the observed enhanced immune response in the case of CNE nanoconjugates as opposed to IFA or GNP nanoconjugates.

However, smaller antigen-CNE nanoconjugates eliciting higher antibody titers remain unresolved. This observed trend in the humoral response of CNE nanoconjugates could be attributed to the surface properties of CNE nanoconjugates. Since 54kDa protein is more hydrophobic and larger, CNE54 will have a lesser exposed surface of bare CNE compared to CNE26. This results in a lower probability of interaction of CNE54 with immune receptors recognizing chitosan than CNE26. In particular, we can conclude that smaller antigen-CNE nanoconjugates formulations can generate efficient cellular and humoral immune response.

4. Conclusions

This study compares immune responses generated in mice by immunizing two different-sized truncated HEV ORF2 proteins with gold and chitosan nanoconjugates. Both CNE and GNP nanoconjugates can induce an effective immune response against the virus. The two HEV ORF2 immunogens used in the study show different immune responses with different nanomaterials. The larger protein shows a better response with metallic nanoparticles than smaller proteins. , The immune response of GNP-protein nanoconjugate, was observed to be controlled by two factors –the immunogenicity of the protein itself and the size of the nanoconjugate. However, immune response for CNE26 was found to be significantly greater than CNE54 (twice) and almost 3 times that of GNP26 and IFA26 conjugates. The exact mechanism/reason for the observed trend in CNE nanoconjugates needs to be explored further. We conclude that chitosan nanomaterials are better adjuvants and elicit an efficient immune response if conjugated with smaller proteins.

Funding

This research was not supported by any external funding.

Acknowledgments

DR is grateful to the Jaypee Institute of Information Technology for research and infrastructure facilities. The authors would like to thank AIIMS, New Delhi, for providing an animal facility and CIF facility Jamia Millia Islamia for Zeta potential, and Zeta size for that was essential for current research. DR acknowledges the INSPIRE fellowship and contingency grant(IF150454) by DST, Government of India. The support extended by Mr. Sonu Kumar during animal studies is also duly acknowledged.

Conflicts of Interest

The authors declare that there is no conflict of interest.

References

1. Ogholikhan, S.; Schwarz, K.B.; Harper, D.M. Hepatitis Vaccines. *Vaccines* **2016**, *4*, https://doi.org/10.3390/vaccines4010006.
2. Seth, A.; Sherman, K. E. Hepatitis E: what we think we know. *Clin. Liver Dis.* **2020**, *15*, S37-S44, https://doi.org/10.1002/CLD.858.
3. Larrue, H.; Abravanel, F.; Péron, J. Hepatitis E, what's the real issue? *Liver Int.* **2020**, *40*, 43–47, https://doi.org/10.1111/liv.14351.

4. Kar, P.; Karna, R. A Review of the Diagnosis and Management of Hepatitis E. *Curr. Treat. Options Infect.* **2020**, *12*, 310–320, https://doi.org/10.1007/S40506-020-00235-4.
5. Thakur, V.; Ratho, R.K.; Kumar, S.; Saxena, S.K.; Bora, I.; Thakur, P. Viral Hepatitis E and Chronicity: A Growing Public Health Concern. *Front. Microbiol.* **2020,** *11*, https://doi.org/10.3389/fmicb.2020.577339.
6. Goel, A.; Aggarwal, R. Hepatitis E virus vaccines: have they arrived–when, where and for whom? In: *Clin. Dilemmas Viral Liver Dis.* 2nd ed. Foster, G.R.; Reddy, R.; Wiley Blackwell: Hoboken, New Jersey, **2020**; pp. 193-199.
7. Pişkinpaşa, N.; Karasakal, Ö.F. Introduction to Vaccination. In: *Synthetic Peptide Vaccine Models.* 1st ed. Mesut, K. CRC Press, Boca Raton, **2021**; pp. 10–25.
8. Gherardi, R.K.; Coquet, M.; Cherin, P.; Belec, L.; Moretto, P.; Dreyfus, P.A.; Pellissier, J.-F.; Chariot, P.; Authier, F.-J. Macrophagic myofasciitis lesions assess long-term persistence of vaccine-derived aluminium hydroxide in muscle. *Brain* **2001**, *124*, 1821-1831, https://doi.org/10.1093/brain/124.9.1821.
9. Petrovsky, N.; Aguilar, J.C. Vaccine adjuvants: current state and future trends. *Immunol. Cell Biol.* **2004**, *82*, 488–496, https://doi.org/10.1111/J.0818-9641.2004.01272.X.
10. Butkovich, N.; Li, E.; Ramirez, A.; Burkhardt, A.M.; Wang, S.W. Advancements in protein nanoparticle vaccine platforms to combat infectious disease. *Wiley Interdiscip. Rev. Nanomed. Nanobiotechnol.* **2021**, *13*, https://doi.org/10.1002/WNAN.1681.
11. Zhao, L.; Seth, A.; Wibowo, N.; Zhao, C.X.; Mitter, N.; Yu, C.; Middelberg, A.P.J. Nanoparticle vaccines. *Vaccine* **2014**, *32*, 327–337, https://doi.org/10.1016/j.vaccine.2013.11.069.
12. AbdelAllah, N.H.; Gaber, Y.; Rashed, M.E.; Azmy, A.F.; Abou-Taleb, H.A.; AbdelGhani, S. Alginate-coated chitosan nanoparticles act as effective adjuvant for hepatitis A vaccine in mice. *Int. J. Biol. Macromol.* **2020**, *152*, 904–912, https://doi.org/10.1016/j.ijbiomac.2020.02.287.
13. Lugade, A.A.; Bharali, D.J.; Pradhan, V.; Elkin, G.; Mousa, S.A.; Thanavala, Y. Single low-dose un-adjuvanted HBsAg nanoparticle vaccine elicits robust, durable immunity. *Nanomedicine Nanotechnology, Biol. Med.* **2013**, *9*, 923-934, https://doi.org/10.1016/j.nano.2013.03.008.
14. Karthick Raja Namasivayam, S.; Nishanth, A.N.; R S, A.B.; Nivedh, K.; Syed, N.H.; R, R.S. Hepatitis B-surface antigen (HBsAg) vaccine fabricated chitosan-polyethylene glycol nanocomposite (HBsAg-CS-PEG-NC) preparation, immunogenicity, controlled release pattern, biocompatibility or non-target toxicity. *Int. J. Biol. Macromol.* **2020**, *144*, 978–994, https://doi.org/10.1016/j.ijbiomac.2019.09.175.
15. Wei, W.; Behloul, N.; Wang, W.; Baha, S.; Liu, Z.; Shi, R.; Meng, J. Chitosan Nanoparticles Loaded with Truncated ORF2 Protein as an Oral Vaccine Candidate against Hepatitis E. *Macromol. Biosci.* **2021**, *21*, 2000375. https://doi.org/10.1002/mabi.202000375.
16. Tao, W.; Zheng, H.-Q.; Fu, T.; He, Z.-J.; Hong, Y. N-\(2-hydroxy\) propyl-3-trimethylammonium chitosan chloride: An immune-enhancing adjuvant for hepatitis E virus recombinant polypeptide vaccine in mice. *Hum. Vaccin. Immunother.* **2017**, *13*, 1818–1822, https://doi.org/10.1080/21645515.2017.1331191.
17. El-Sissi, A.F.; Mohamed, F.H.; Danial, N.M.; Gaballah, A.Q.; Ali, K.A. Chitosan and chitosan nanoparticles as adjuvant in local Rift Valley Fever inactivated vaccine. *3 Biotech* **2020**, *10*, https://doi.org/10.1007/s13205-020-2076-y.
18. Manish, M.; Rahi, A.; Kaur, M.; Bhatnagar, R.; Singh, S. A Single-Dose PLGA Encapsulated Protective Antigen Domain 4 Nanoformulation Protects Mice against Bacillus anthracis Spore Challenge. *PLoS One* **2013**, *8*, https://doi.org/10.1371/journal.pone.0061885.
19. Thomas, C.; Rawat, A.; Hope-Weeks, L.; Ahsan, F. Aerosolized PLA and PLGA Nanoparticles Enhance Humoral, Mucosal and Cytokine Responses to Hepatitis B Vaccine. *Mol. Pharm.* **2011**, *8*, 405–415, https://doi.org/10.1021/mp100255c.
20. Singh, J.; Pandit, S.; Bramwell, V.W.; Alpar, H.O. Diphtheria toxoid loaded poly-(ε-caprolactone) nanoparticles as mucosal vaccine delivery systems. *Methods* **2006**, *38*, 96–105, https://doi.org/10.1016/j.ymeth.2005.11.003.
21. Abraham, E. Intranasal immunization with bacterial polysaccharide containing liposomes enhances antigen-specific pulmonary secretory antibody response. *Vaccine* **1992**, *10*, 461–468, https://doi.org/10.1016/0264-410X(92)90395-Z.
22. Quach, Q.H.; Ang, S.K.; Chu, J.H.J.; Kah, J.C.Y. Size-dependent neutralizing activity of gold nanoparticle-based subunit vaccine against dengue virus. *Acta Biomater.* **2018**, *78*, 224–235, https://doi.org/10.1016/j.actbio.2018.08.011.
23. Farfán-Castro, S.; García Soto, M.J.; Comas-García, M.; Arévalo-Villalobos, J.I.; Palestino, G.; González-Ortega, O.; Rosales-Mendoza, S. Synthesis and immunogenicity assessment of a gold nanoparticle conjugate for the delivery of a peptide from SARS-CoV-2. *Nanomedicine Nanotechnology, Biol. Med.* **2021**, *34*, https://doi.org/10.1016/j.nano.2021.102372.
24. Mohammed, I.A.; Al-Gawhari, F.J. Gold Nanoparticle: Synthesis, Functionalization, Enhancement, Drug Delivery and Therapy: A Review. *Sys. Rev. Pharm.* **2020**, *11*, 888-910.
25. Pusic, K.; Aguilar, Z.; McLoughlin, J.; Kobuch, S.; Xu, H.; Tsang, M.; Wang, A.; Hui, G. Iron oxide nanoparticles as a clinically acceptable delivery platform for a recombinant blood-stage human malaria vaccine. *FASEB J.* **2013,** *27*, 1153–1166, https://doi.org/10.1096/fj.12-218362.

26. Scott, G.B.; Williams, H.S.; Marriott, P.M. The phagocytosis of colloidal particles of different sizes. *Br. J. Exp. Pathol.* **1967**, *48*.
27. Singer, J.M.; Adlersberg, L.; Sadek, M. Long-term observation of intravenously injected colloidal gold in mice. *J. Reticuloendothel Soc.* **1972**, *12*, 658-7.
28. Hardonk, M.J.; Harms, G.; Koudstaal, J. Zonal heterogeneity of rat hepatocytes in the in vivo uptake of 17 nm colloidal gold granules. *Histochem.* **1985**, *83*, 473–477, https://doi.org/10.1007/BF00509211.
29. Renaud, G.; Hamilton, R.L.; Havel, R.J. Hepatic metabolism of colloidal gold-low-density lipoprotein complexes in the rat: Evidence for bulk excretion of lysosomal contents into bile. *Hepatology* **1989**, *9*, 380–392, https://doi.org/10.1002/HEP.1840090307.
30. Nam, J.; Son, S.; Moon, J.J. Adjuvant-Loaded Spiky Gold Nanoparticles for Activation of Innate Immune Cells. *Cell. Mol. Bioeng.* **2017**, *10*, 341–355. https://doi.org/10.1007/S12195-017-0505-8.
31. Sekimukai, H.; Iwata-Yoshikawa, N.; Fukushi, S.; Tani, H.; Kataoka, M.; Suzuki, T.; Hasegawa, H.; Niikura, K.; Arai, K.; Nagata, N. Gold nanoparticle-adjuvanted S protein induces a strong antigen-specific IgG response against severe acute respiratory syndrome-related coronavirus infection, but fails to induce protective antibodies and limit eosinophilic infiltration in lungs. *Microbiol. Immunol.* **2020**, *64*, 33–51, https://doi.org/10.1111/1348-0421.12754.
32. Shukla, R.; Bansal, V.; Chaudhary, M. Biocompatibility of gold nanoparticles and their endocytotic fate inside the cellular compartment: a microscopic overview. *Langmuir* **2005**, *21*, 10644–10654, https://doi.org/10.1021/LA0513712.
33. Yen, H.J.; Hsu, S.H.; Tsai, C.L. Cytotoxicity and immunological response of gold and silver nanoparticles of different sizes. *Small* **2009**, *5*, 1553–1561, https://doi.org/10.1002/SMLL.200900126.
34. Wang, H.; Ding, Y.; Su, S.; Meng, D.; Mujeeb, A.; Wu, Y.; Nie, G. Assembly of hepatitis e vaccine by ': In situ ' growth of gold clusters as nano-adjuvants: An efficient way to enhance the immune responses of vaccination. *Nanoscale Horizons* **2016**, *1*, 394–398, https://doi.org/10.1039/c6nh00087h.
35. Dykman, L.A.; Staroverov, S.A.; Fomin, A.S.; Khanadeev, V.A.; Khlebtsov, B.N.; Bogatyrev, V.A. Gold nanoparticles as an adjuvant: Influence of size, shape, and technique of combination with CpG on antibody production. *Int. Immunopharmacol.* **2018**, *54*, 163–168, https://doi.org/10.1016/j.intimp.2017.11.008.
36. Gregory, A.E.; Titball, R.; Williamson, D. Vaccine delivery using nanoparticles. *Front. Cell. Infect. Microbiol.* **2013**, *23*, https://doi.org/10.3389/fcimb.2013.00013.
37. Niikura, K.; Matsunaga, T.; Suzuki, T.; Kobayashi, S.; Yamaguchi, H.; Orba, Y.; Kawaguchi, A.; Hasegawa, H.; Kajino, K.; Ninomiya, T.; Ijiro, K.; Sawa, H. Gold nanoparticles as a vaccine platform: Influence of size and shape on immunological responses in vitro and in vivo. *ACS Nano* **2013**, *7*, 3926–3938, https://doi.org/10.1021/nn3057005.
38. Xu, L.; Liu, Y.; Chen, Z.; Li, W.; Liu, Y.; Wang, L.; Liu, Y.; Wu, X.; Ji, Y.; Zhao, Y.; Ma, L.; Shao, Y.; Chen, C. Surface-engineered gold nanorods: Promising DNA vaccine adjuvant for HIV-1 treatment. *Nano Lett.* **2012**, *12*, 2003–2012, https://doi.org/10.1021/nl300027p.
39. Rani, D.; Nayak, B.; Srivastava, S. Immunogenicity of gold nanoparticle-based truncated ORF2 vaccine in mice against Hepatitis E virus. *3 Biotech* **2021**, *11*, https://doi.org/10.1007/s13205-020-02573-y.
40. Li, X.; Min, M.; Du, N.; Gu, Y.; Hode, T.; Naylor, M.; Chen, D.; Nordquist, R.E.; Chen, W.R. Chitin, Chitosan, and Glycated Chitosan Regulate Immune Responses: The Novel Adjuvants for Cancer Vaccine. *Clin. Dev. Immunol.* **2013**, *2013*, https://doi.org/10.1155/2013/387023.
41. Vasiliev, Y.M. Chitosan-based vaccine adjuvants: incomplete characterization complicates preclinical and clinical evaluation. *Expert Rev. Vaccines* **2015**, *14*, 37–53, https://doi.org/10.1586/14760584.2015.956729.
42. Guo, J.; Sun, X.; Yin, H.; Wang, T.; Li, Y.; Zhou, C.; Zhou, H.; He, S.; Cong, H. Chitosan microsphere used as an effective system to deliver a linked antigenic peptides vaccine protect mice against acute and chronic Toxoplasmosis. *Front. Cell. Infect. Microbiol.* **2018**, *8*, https://doi.org/10.3389/fcimb.2018.00163.
43. Chua, B.Y.; Al Kobaisi, M.; Zeng, W.; Mainwaring, D.; Jackson, D.C. Chitosan microparticles and nanoparticles as biocompatible delivery vehicles for peptide and protein-based immunocontraceptive vaccines. *Mol. Pharm.* **2012**, *9*, 81–90, https://doi.org/10.1021/mp200264m.
44. Zaharoff, D.A.; Rogers, C.J.; Hance, K.W.; Schlom, J.; Greiner, J.W. Chitosan solution enhances both humoral and cell-mediated immune responses to subcutaneous vaccination. *Vaccine* **2007**, *25*, 2085–2094, https://doi.org/10.1016/j.vaccine.2006.11.034.
45. Rani, D.; Saxena, R.; Nayak, B.; Srivastava, S. Cloning and expression of truncated ORF2 as a vaccine candidate against hepatitis E virus. *3 Biotech* **2018**, *8*, https://doi.org/10.1007/s13205-018-1437-2.
46. Medhi, R.; Srinoi, P.; Ngo, N.; Tran, H.-V.; Lee, T.R. Nanoparticle-Based Strategies to Combat COVID-19. *ACS Appl. Nano Mater.* **2020**, *3*, 8557–8580, https://doi.org/10.1021/acsanm.0c01978.
47. Bastús, N.G.; Sánchez-Tilló, E.; Pujals, S.; Farrera, C.; Kogan, M.J.; Giralt, E.; Celada, A.; Lloberas, J.; Puntes, V. Peptides conjugated to gold nanoparticles induce macrophage activation. *Mol. Immunol.* **2009**, *46*, 743–748, https://doi.org/10.1016/j.molimm.2008.08.277.
48. Bancos, S.; Stevens, D.L.; Tyner, K.M. Effect of silica and gold nanoparticles on macrophage proliferation, activation markers, cytokine production, and phagocytosis in vitro. Int. J. Nanomedicine **2014**, *10*, 183–206, https://doi.org/10.2147/IJN.S72580.

49. Lacerda, S.H.D.P.; Park, J.J.; Meuse, C.; Pristinski, D.; Becker, M.L.; Karim, A.; Douglas, J.F. Interaction of Gold Nanoparticles with Common Human Blood Proteins. *ACS Nano* **2009**, *4*, 365–379, https://doi.org/10.1021/NN9011187.
50. Chen, Y.S.; Hung, Y.C.; Lin, W.H.; Huang, G.S. Assessment of gold nanoparticles as a size-dependent vaccine carrier for enhancing the antibody response against synthetic foot-and-mouth disease virus peptide. *Nanotechnology* **2010**, *21*, https://doi.org/10.1088/0957-4484/21/19/195101.
51. Bueter, C.L.; Lee, C.K.; Rathinam, V.A.K.; Healy, G.J.; Taron, C.H.; Specht, C.A.; Levitz, S.M. Chitosan but Not Chitin Activates the Inflammasome by a Mechanism Dependent upon Phagocytosis*. *J. Biol. Chem.* **2011**, *286*, 35447–35455, https://doi.org/10.1074/JBC.M111.274936.